Origin of ferromagnetism in semiconducting $(\mathrm{In_{1-x-y}Fe_xCu_y})_2\mathrm{O_{3-\sigma}}$

Z. G. Yu,[1] Jun He,[1] Shifa Xu,[1] Qizhen Xue,[2] O. M. J. van't Erve,[3] B. T. Jonker,[3] M. A. Marcus,[4] Young K. Yoo,[2] Shifan Cheng,[2] and Xiao-dong Xiang[1,2,*]

[1]*SRI International, 333 Ravenswood Avenue, Menlo Park, California 94025, USA*
[2]*Intematix Corporation, 46410 South Fremont Boulevard, Fremont, California 94538, USA*
[3]*Naval Research Laboratory, 4555 Overlook Avenue SW, Washington, DC 20375, USA*
[4]*Advanced Light Source, Lawrence Berkeley National Laboratory, 1 Cyclotron Road, Berkeley, California 94720, USA*

We systematically measure and analyze x-ray absorption fine structure and the anomalous Hall effect of recently discovered room-temperature ferromagnetic semiconductor thin films, $(\mathrm{In_{1-x-y}Fe_xCu_y})_2\mathrm{O_{3-\sigma}}$. The x-ray fine structure demonstrates that divalent Fe ions exist in ferromagnetic samples but not in nonmagnetic ones, suggesting a mobile-electron-mediated ferromagnetism. The anomalous Hall behavior is found to be consistent with that of ferromagnets, in which carriers are delocalized, but qualitatively different from that of double-exchange manganites, in which carriers are bound to magnetic ions, confirming that the ferromagnetism in $(\mathrm{In_{1-x-y}Fe_xCu_y})_2\mathrm{O_{3-\sigma}}$ is mediated by mobile electrons.

I. INTRODUCTION

Room-temperature ferromagnetic semiconductors have attracted great attention because of their potential applications in spintronics.[1] Many promising candidates with high Curie temperatures have been discovered.[2–12] Recently we used a combinatorial approach[13,14] and identified a ferromagnetic n-type semiconductor system $(\mathrm{In_{1-x-y}Fe_xCu_y})_2\mathrm{O_{3-\sigma}}$ (IFCO).[15,16] The Curie temperature of this material exceeds room temperature and the concentration x of Fe ions in the host lattice, $\mathrm{In_2O_3}$, can be as high as 20%. Possible impurity magnetic phases in IFCO have been ruled out via extensive structural, magnetic, and magnetotransport studies on both bulk and thin-film samples.[15,16] While the room-temperature ferromagnetism in this material is robustly established, its origin and the underlying physics remain elusive. Possible mechanisms proposed for ferromagnetic semiconductors fall into two categories: carrier mediated or superexchange. In carrier-mediate models (e.g., the Ruderman-Kittle-Kasuya-Yosida and the Zener models),[17–19] the coupling between magnetic ions is achieved through electrons in the conduction band or holes in the valence band. In superexchange models (e.g., the double-exchange model),[20–23] the coupling is achieved through anions between the magnetic ions. The key difference between these two mechanisms is that the magnetic coupling is mediated by mobile carriers in the former but localized ones in the latter.

To uncover which type mechanism leading to ferromagnetism in IFCO, we carried out detailed measurements of x-ray absorption fine structures and the anomalous Hall effect (AHE) in IFCO films at representative compositions. We focus on these two measurements because the ferromagnetism originates microscopically from atomic bonding and ion valence, which can be discerned by the x-ray absorption near-edge structure (XANES) and extended x-ray absorption edge fine structure (EXAFS), and manifests itself macroscopically in collective transport, which can be reliably measured by the AHE. Based on the lattice structure and valence information obtained from XANES and EXAFS, we con-

clude that the presence of divalent Fe ions, or equivalently, mobile electrons, is requisite for IFCO to be ferromagnetic, suggesting a carrier-mediated ferromagnetism. The notion of mobile-electron-mediated ferromagnetism in IFCO is reinforced by the AHE measurements, which show that the carrier transport behavior is more like band conduction as in ferromagnets than hopping conduction as in double-exchange manganites. In addition, these measurements further confirm, both microscopically and macroscopically, that the ferromagnetism of IFCO is intrinsic rather than from magnetic impurities.

II. RESULTS AND DISCUSSIONS

IFCO thin films with specific compositions were grown on (0001) $\alpha-\mathrm{Al_2O_3}$ substrate by pulsed laser deposition using targets of corresponding stoichiometry. Different flow rates of high purity $\mathrm{O_2}$ gas are introduced to vary the $\mathrm{O_2}$ partial pressures for thin film deposition. A KrF excimer laser ($\lambda=248$ nm) with a beam energy density of $2.4-2.8$ J/cm² was used at a repetition rate of 10 Hz and pulse duration of 10 ns. Films with a typical thickness of 0.5 μm, as measured by a Dektak 3 profilometer, were deposited at a rate of 2.8 Å/s. The substrates were heated during thin film deposition. XANES and EXAFS data were collected at beamline 10.3.2 at the Advanced Light Source,[24] which produces a beam of 15×7 μm. Data at the Fe K-edge were taken in fluorescence using a seven-element Ge detector at 10° grazing incidence. Counts from each detector element were recorded separately to help the treatment of substrate Bragg peaks. Hall measurements were performed by using a Hall bar in a cryostat equipped with a 9 T superconducting magnet.

Figure 1(a) depicts XANES spectrum, $\mu(E)$, for five representative samples, three IFCO thin-film samples with $x=0.15$ and nominal 2% Cu but grown under different $\mathrm{O_2}$ partial pressures, a bulk $(\mathrm{In_{0.94}Fe_{0.06}})_2\mathrm{O_3}$ sample, a thin film of $\mathrm{Fe_3O_4}$, and a thin film of $\mathrm{Fe_2O_3}$.[25] Cu doping was found not to be directly responsible for the magnetism of IFCO.[16,26]
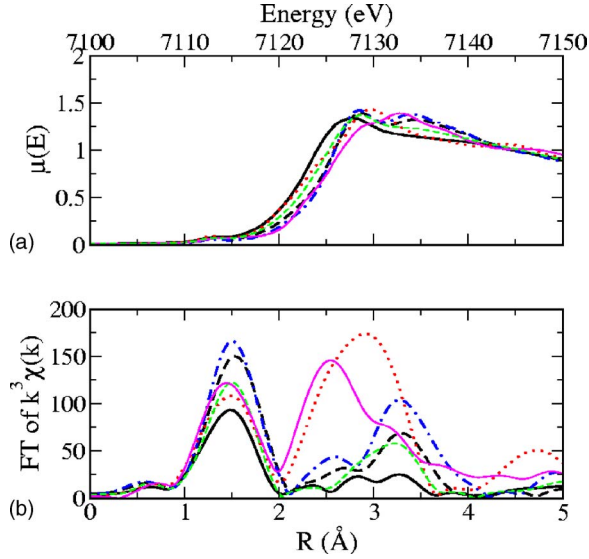
FIG. 1. (Color online) XANES (a) and Fourier transform of k^3 weighted EXAFS (b) spectra of thin-film samples of IFCO with $x=0.15$ grown under the O_2 partial pressures of 10^{-7}, 9×10^{-6}, and 5×10^{-4} Torr. Solid (black), thin-dashed (green), and dashed (black) lines are for the sample of the low, medium, and high O_2 partial pressures. The spectra of $(In_{0.94}Fe_{0.06})_2O_3$ (dotted-dashed lines, blue), Fe_3O_4 (dotted lines, red), and Fe_2O_3 (thin solid lines, magenta) are also plotted for comparison.

Our magnetization measurements indicate that the IFCO sample grown under a high O_2 partial pressure $(5 \times 10^{-4}$ Torr$)$ and $(In_{0.94}Fe_{0.06})_2O_3$ are nonmagnetic, while the IFCO sample grown under a low O_2 partial pressure $(10^{-7}$ Torr$)$ is strongly magnetic, 0.8 μ_B/Fe at room temperature.[27] The IFCO sample grown under a medium O_2 partial pressure $(9 \times 10^{-7}$ Torr$)$ is weakly magnetic, 0.1 μ_B/Fe at room temperature.

Noting that in Fe_2O_3 only Fe^{3+} ions exist, whereas in Fe_3O_4 one-third of the Fe ions are reduced (Fe^{2+}), we see from Fig. 1(a) that the XANES edges of the $(In_{0.94}Fe_{0.06})_2O_3$ and high-O_2-partial-pressure samples, which both are non-magnetic, coincide with that of Fe_2O_3, indicating that only Fe^{3+} ions exist in these samples. On the other hand, the XANES edge of the low-O_2-partial-pressure sample, which is highly magnetic, appears at a lower energy and overlaps with that of Fe_3O_4, indicating a significant amount of Fe^{2+} in the sample with a similar Fe^{2+}/Fe^{3+} ratio as in Fe_3O_4. The XANES edge of the medium-O_2-partial-pressure sample lies between those of the high- and low-O_2-partial-pressure samples, suggesting that Fe^{2+} ions are present in the sample but fewer than in the low-O_2-partial-pressure sample. The unmixed trivalence of Fe ions in the stoichiometric $(In_{0.94}Fe_{0.06})_2O_3$ is a direct consequence of Fe substitution into In sites of In_2O_3, which is unambiguously shown in the EXAFS data (see below). The dependence of valence on the O_2 partial pressure can be described by the following reaction formula:

$$O_O \rightarrow V_{O\cdot\cdot} + 2e + \tfrac{1}{2}O_2, \qquad (1)$$
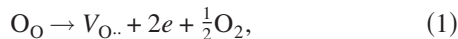
where O_O represents an oxygen ion, $V_{O\cdot\cdot}$ a positively charged oxygen vacancy in the lattice, and e an electron. Using the

TABLE I. Structural parameters obtained from FEFF8.1 fitting for the same materials as in Fig. 1. The fits were done assuming a single Fe-O distance. N is the averaged coordination number, R_{Fe-O} is the Fe-O bond length, and $\Delta\sigma^2$ is the Debye-Waller factor. Error bars are 0.02 Å for R_{Fe-O} and 15% for N.

Sample	N	R_{Fe-O} (Å)	$\Delta\sigma^2$ $(\times 10^{-4}$ Å)
$(In_{0.94}Fe_{0.06})_2O_3$	5.3	2.03	49.7
High-O_2-partial-pressure	5.3	2.03	46.7
Medium-O_2-partial-pressure	4.7	2.03	19.4
Low-O_2-partial-pressure	4.4	1.97	15.5
Fe_3O_4	4.6	1.99	85.9
Fe_2O_3	5.2	1.98	83.0

charge neutrality condition (the number of electrons is 2 times the number of oxygen vacancies), one obtains that in equilibrium, both the electron and Fe^{2+} densities depend on the O_2 partial pressure, P_{O_2}, via $n \propto P_{O_2}^{-1/6}$.[28,29] From Eq. (1), oxygen deficiency will be balanced by Fe^{2+} ions and mobile electrons, whose density increases as the O_2 partial pressure decreases. The observed correlation between valence and magnetization suggests that the presence of Fe^{2+} ions (or mobile electrons) is required for IFCO to be magnetic.

We plot the Fourier transform of $k^3\chi(k)$ [$\chi(k) \equiv (\mu - \mu_0)/\mu_0$ with μ_0 being the background absorption, is the extracted EXAFS oscillation] of these samples in Fig. 1(b) and list their structural parameters in Table I from FEFF8.1 fitting.[30,31] The EXAFS spectra were analyzed according to a standard procedure[31–33] and the Fourier-transform cutoff is $k=11.5$ Å^{-1}. For an informative comparison between samples, we fitted the first shell by assuming a single Fe-O distance (strictly speaking, the assumption is not accurate for Fe_3O_4, in which there are two kinds of Fe-O bonds with lengths 1.886 Å and 2.0602 Å, respectively). The In atoms in the host In_2O_3 are coordinated by six oxygens forming distorted octahedra. There are two inequivalent In sites, one of which (site 1) has six equal In-O distance (2.21 Å), and the other (site 2) having four different distances (2.09–2.22 Å). In both sites, the neighboring octahedra are shared with either corners or edges, resulting in two distinct In-In distances, 3.35 Å and 3.83 Å.[34] From Fig. 1(b), $(In_{0.94}Fe_{0.06})_2O_3$ also has two Fe-In distances in the second shell (2–4 Å), suggesting Fe is substituted into In sites, which is corroborated by the FEFF simulations of Fe substituted into In site 2 (the data agree better with a simulation of site 2 than site 1).[25] The high-O_2-partial-pressure sample has very similar XANES and EXAFS spectra to $(In_{0.94}Fe_{0.06})_2O_3$ with slightly attenuated intensity, implying that they essentially have the same lattice structure. This conclusion is bolstered by the FEFF fitting, which shows that the two materials have virtually identical local structure with the Fe-O bond length $R_{Fe-O}=2.03$ Å, close to that of In_2O_3 crystal (2.1–2.2 Å),[34] and the averaged coordination $N=5.3$, approximately equal to 6 within experimental uncertainty. That the Fe-O distance is shorter than the In-O distance may be explained by the fact that Fe^{3+} is smaller than In^{3+}.

However, the second-shell EXAFS of the low-O_2-partial-pressure sample is noticeably different from that

of the high-O_2-partial-pressure one: The intensity is considerably reduced and the first peak at 2.7 Å splits into two. The peak splitting suggests significant lattice distortion in the low-O_2-partial-pressure sample. This is understandable by noticing that reduced Fe ions in the sample, as seen in XANES, are accompanied by charged oxygen vacancies, which can cause a considerable distortion in the host In_2O_3 lattice. This distortion may change the local lattice structure to one with a lower symmetry and thus reduce the intensity of the higher shell EXAFS. The considerably reduced R_{Fe-O} and N confirm the existence of oxygen vacancies and the significantly distorted lattice and further suggest a strong deviation in the low-O_2-partial-pressure sample from the simply substitutional structure as in the high-O_2-partial-pressure sample. The shorter Fe-O distance may be due to the reduction of oxygen-oxygen repulsion forces that occurs when oxygen vacancies are introduced, or may reflect the existence of Fe^{2+} in tetrahedral sites, presumably associated with oxygen vacancies. It is interesting to note that if the reduction of N in the low-O_2-partial-pressure sample is assumed to be due solely to the oxygen vacancies, 17% $[(5.3-4.4)/5.3]$ oxygen ions surrounding Fe will be vacant, which means 34% Fe are divalent, according to Eq. (1). This is in agreement with the amount of Fe^{2+} (1/3) estimated from the XANES. The EXAFS of the medium-O_2-partial-pressure sample, again, falls between those of the high- and low-O_2-partial-pressure samples, suggesting that its lattice distortion is less severe and the oxygen vacancies are fewer than those in the low-O_2-partial-pressure sample, which is also reflected by the fitted values of R_{Fe-O} and N in Table I.

Hence both XANES and EXAFS suggest a connection between the presence of Fe^{2+} ions and the ferromagnetism in IFCO. The disparate magnetizations in the systems with and without Fe^{2+} ions indicates that mobile electrons, which only exist in systems containing Fe^{2+} ions, are required to make IFCO magnetic. This observation is consistent with the ferromagnetism mediated by delocalized carriers.[17–19] We emphasize that the observed ferromagnetism in IFCO cannot be attributed to Fe_3O_4, for (1) fits to the second-shell region by assuming the sample is a combination of Fe_3O_4 and the high-O_2-partial-pressure IFCO or $(In_{0.94}Fe_{0.06})_2O_3$ reveal that no more than 5% of Fe is in the form of Fe_3O_4, which is too little to account for the strong magnetization, $0.8\mu_B$/Fe at room temperature (at least 60% Fe in the form of Fe_3O_4, whose saturated magnetization is $1.35\mu_B$/Fe, would be needed), (2) the EXAFS spectra of IFCO is quite different from that of Fe_3O_4. Nor can the ferromagnetism in IFCO come from Fe_2O_3, according to their dissimilar XANES and EXAFS data.

Because mobile electrons and localized ones are expected to lead to very different magnetotransport behaviors, we perform a detailed AHE study to further understand the ferromagnetism in IFCO. The AHE depends linearly on the macroscopic magnetization of a sample, and therefore plays an important role in establishing intrinsic ferromagnetism in a system.[35] The Hall resistivity ρ_{xy} in magnetic materials can be expressed by

$$\rho_{xy} = R_0 B + \mu_0 R_s M. \tag{2}$$

The first term is the ordinary Hall effect and the second is the AHE. Here B is the internal magnetic induction, R_0 the or-
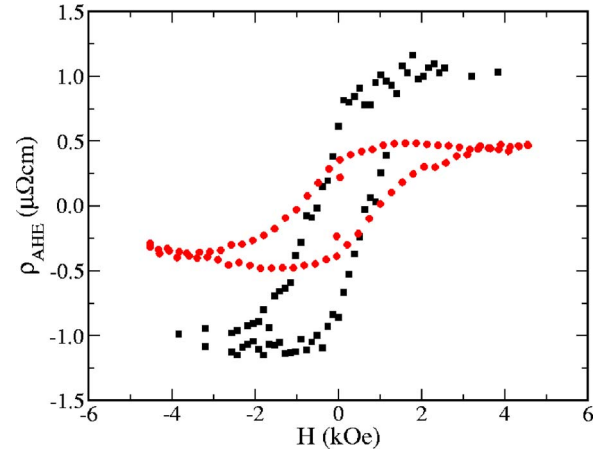
FIG. 2. (Color online) Room-temperature anomalous Hall resistivity as a function of the applied magnetic field in the two IFCO thin films with $x=0.15$. Squares (black) and circles (red) are for the first and the second samples, which were grown at 550 °C under 10^{-7} Torr O_2 partial pressure and at 575 °C under 5×10^{-7} Torr O_2 partial pressure, respectively.

dinary Hall coefficient, M the magnetization, μ_0 the vacuum permeability, and R_s the anomalous Hall coefficient. Figure 2 shows the anomalous Hall resistivity ρ_{AHE}, which follows hysteresis loops similar to those of measured M-H curves, of two ferromagnetic IFCO thin films. The two samples have the same Fe composition ($x=0.15$) but were grown under slightly different conditions, which ensure that the two samples have a similar lattice structure but possible different carrier density. Both thin film samples are found to be n type. The carrier density n is deduced from the Hall coefficient R_0, $n=1/eR_0$, and the Hall mobility is obtained from $\mu_H = R_0/\rho_{xx}$, where ρ_{xx} is the sheet resistivity. The transport properties of these two samples are summarized in Table II.

To place these results in perspective, we briefly reiterate the AHE in two limiting cases. One is conventional ferromagnets, where transport is via band conduction (mobile electrons), the other double-change manganites like $La_{1-x}Ca_xMnO_3$, where the conduction is via electron hopping (localized electrons). In the ferromagnets, the magnetism can be reasonably described by the Stoner iterant-electron magnetism model and the AHE mainly comes from the so-called "side-jump" mechanism,[36,37] which is recently found to be also responsible for the observed AHE in Mn-doped III-V ferromagnetic semiconductors.[38] If we define another AHE coefficient, $\sigma_{AH} \equiv \sigma_{xy}^{AHE}/\mu_0 M$, where σ_{xy}^{AHE} is the anomalous part of the Hall conductivity $\sigma_{xy} \equiv \rho_{xy}/(\rho_{xy}^2+\rho_{xx}^2)$, the side-jump contribution to the AHE can be written as[37,39,40]

$$\sigma_{AH} = \gamma_1 n, \tag{3}$$

where n is the carrier density and the prefactor γ_1 depends on the Compton wavelength and the Planck's constant but not impurity concentrations or potentials. Thus one would expect that σ_{AH} is proportional to the carrier density in a ferromagnet.

In the strong localization regime, the Hall resistivity has a classical form, $\rho_{xy} \sim B/ne$,[42,43] which can be obtained by

TABLE II. Room-temperature transport properties of the same two ferromagnetic IFCO thin films as in Fig. 2.

Sample	R_0 (10^{-2} cm^3/C)	μ_H (cm^2/Vs)	n (10^{20} cm^{-3})	R_s (10^{-1} cm^3/C)	ρ_{xx} (10^{-3} Ω cm)	σ_{AH} (10^3 cm/Ω^2 C)
I	−19.1	32.2	0.33	2.8	5.791	8.35
II	−44.4	63.42	0.14	2.268	7	4.63

considering hoppings among small triads. The magnetic flux in the area enclosed by a triad gives rise to an Aharonov-Bohm phase, which generates a Hall current. For a magnetic system with hopping conduction, such as double-exchange manganite $La_{1-x}Ca_xMnO_3$, this magnetic flux is proportional to the magnetization, i.e., the core spin inside the triad,[41,44] and one would expect[41]

$$R_s = \gamma_2/n, \tag{4}$$

where the prefactor γ_2 is independent of impurity concentrations and potentials. For systems where the AHE arises from magnetic impurities,[45] the classical form of the Hall resistivity still holds and it follows that Eq. (4) is also valid.

From Table II, we see that the sample with a smaller n has a smaller R_s, which is qualitatively different from the behavior of Eq. (4), implying that the AHE in IFCO cannot be described by electron hoppings in the double-exchange model or attributed to magnetic impurities. On the other hand, we see that σ_{AH} is approximately proportional to the carrier density, consistent with the behavior expected for a ferromagnet, where electrons are mobile and delocalized. Thus the AHE data further confirm that the exchange couplings between magnetic ions in IFCO are mediated by mobile electrons rather than localized ones.

III. CONCLUSIONS

In summary, we have systematically measured and analyzed x-ray absorption fine structures and the AHE of recently discovered IFCO room-temperature ferromagnetic semiconductor thin films, to identify their origin of ferromagnetism. The XANES and EXAFS data exhibit a strong correlation between the presence of Fe^{2+} ions and the ferromagnetism in IFCO. The measured AHE behavior of IFCO is found to be consistent with band conduction as in ferromagnets but incompatible with hopping conduction as in double-exchange manganites. The complementary microscopic and macroscopic measurements lead us to conclude that the ferromagnetism in semiconducting IFCO originates from the mobile-electron-mediated coupling between Fe ions and further confirm the intrinsicness of the ferromagnetism in IFCO.

*Corresponding author, xdxiang@intematix.com

[1] S. A. Wolf, D. D. Awschalom, R. A. Buhrman, J. M. Daughton, S. von Molnár, M. L. Roukes, A. Y. Chtchelkanova, and D. M. Treger, Science **294**, 1488 (2001).

[2] T. Dietl, H. Ohno, F. Matsukura, J. Cibert, and D. Ferrand, Science **287**, 1019 (2000).

[3] F. Matsukura, H. Ohno, and T. Dietl, in Handbook of magnetic materials, edited by K. H. J. Buschow, 2002, Vol. 14.

[4] Y. Matsumoto, M. Murakami, T. Shono, T. Hasegawa, T. Fukumura, M. Kawasaki, P. Ahmet, T. Chikyow, S. Koshihara, and H. Koinuma, Science **291**, 854 (2001).

[5] Z. J. Wang, W. D. Wang, J. K. Tang, L. D. Tung, L. Spinu, and W. Zhou, Appl. Phys. Lett. **83**, 518 (2003).

[6] S. J. Han, J. W. Song, C. H. Yang, S. H. Park, J. H. Park, Y. H. Jeong, and K. W. Rhie, Appl. Phys. Lett. **81**, 4212 (2002).

[7] D. P. Norton, S. J. Pearton, A. F. Hebard, N. Theodoropoulou, L. A. Boatner, and R. G. Wilson, Appl. Phys. Lett. **82**, 239 (2003).

[8] Y. D. Park, A. T. Hanbicki, S. C. Erwin, C. S. Hellberg, J. M. Sullivan, J. E. Mattson, T. F. Ambrose, A. Wilson, G. Spanos, and B. T. Jonker, Science **295**, 651 (2002).

[9] F. Tsui, L. He, L. Ma, A. Tkachuk, Y. S. Chu, K. Nakajima, and T. Chikyow, Phys. Rev. Lett. **91**, 177203 (2003).

[10] M. L. Reed, N. A. El-Masry, H. H. Stadelmaier, M. K. Ritums, M. J. Reed, C. A. Parker, J. C. Roberts, and S. M. Bedair, Appl. Phys. Lett. **79**, 3473 (2001).

[11] N. Theodoropoulou, A. F. Hebard, M. E. Overberg, C. R. Abernathy, S. J. Pearton, S. N. G. Chu, and R. G. Wilson, Phys. Rev. Lett. **89**, 107203 (2002).

[12] S. Cho, S. Choi, G.-B. Cha, S. C. Hong, Y. Kim, Y. J. Zhao, A. J. Freeman, J. B. Ketterson, B. J. Kim, Y. C. Kim, and B. C. Choi, Phys. Rev. Lett. **88**, 257203 (2002).

[13] X. D. Xiang and I. Takeuchi, *Combinatorial Materials Synthesis* (Marcel Dekker, New York, 2003).

[14] Y. K. Yoo and F. Tsui, MRS Bull. **27**, 316 (2002).

[15] Y. K. Yoo, Q. Xue, H. C. Lee, S. Cheng, X.-D. Xiang, S. Xu, J. He, Y. S. Chu, S. D. Preite, S. E. Lofland, I. Takeuchi, and G. F. Dionne, Appl. Phys. Lett. **86**, 042506 (2005).

[16] J. He, S. Xu, Y. K. Yoo, Q. Xue, H. C. Lee, S. Cheng, X. D.

Xiang, and I. Takeuchi, Appl. Phys. Lett. **86**, 052503 (2005).

[17] See, e. g., C. Kittel, in *Solid State Physics*, Vol. 22, edited by F. Seitz, D. Turnbull, and H. Ehrenreich (Academic, New York, 1968), p. 1.

[18] T. Dietl, A. Haury, and Y. M. d Aubigne, Phys. Rev. B **55**, R3347 (1997).

[19] T. Dietl, H. Ohno, F. Matsukura, J. Cibert, and D. Ferrand, Science **287**, 1019 (2000); T. Dietl, H. Ohno, and F. Matsukura, Phys. Rev. B **63**, 195205 (2001).

[20] P. W. Anderson and H. Hasegawa, Phys. Rev. **100**, 675 (1955).

[21] P. G. De Gennes, Phys. Rev. **118**, 141 (1960).

[22] H. Akai, Phys. Rev. Lett. **81**, 3002 (1998).

[23] M. van Schilfgaarde and O. N. Mryasov, Phys. Rev. B **63**, 233205 (2001).

[24] M. A. Marcus, A. A. MacDowell, R. Celestre, A. Manceau, T. Miller, H. A. Padmore, and R. E. Sublett, J. Synchrotron Radiat. **11**, 239 (2004).

[25] More information on XANES/EXAFS data is available at http://aristotle.sri.com/~zyu/XAS.htm

[26] Our Cu EXAFS analysis indicates that both the low- and high-O_2-partial-pressure samples contain metallic Cu and Cu-O in the first shell at about the bond length of CuO.

[27] A magnetic moment of $1.4\mu_B$ per Fe was detected in the low-O_2-partial-pressure sample at $T=5$ K.

[28] See, e. g., O. T. Sorensen, in *Mass Transport in Solids*, edited by F. Beniere and C. R. A. Catlow (Plenum, New York, 1983), p. 377.

[29] F. A. Kröger and H. J. Vink, in *Solid State Physics*, edited by F. Seitz and D. Turnbull, (Academic, New York, 1956), Vol. 3, p. 307.

[30] A. L. Ankudinov, B. Ravel, J. J. Rehr, and S. D. Conradson, Phys. Rev. B **58**, 7565 (1998).

[31] Software available on Beamline 10.3.2 website, http://xraysweb.lbl.gov/uxas/Beamline/Software/software.htm

[32] P. A. Lee, P. H. Citrin, P. Eisenberger, and B. M. Kincaid, Rev. Mod. Phys. **53**, 769 (1981).

[33] E. A. Stern, B. A. Bunker, and S. M. Heald, Phys. Rev. B **21**, 5521 (1980).

[34] M. Von Betzl, W. Hase, K. Kleinstuck, and J. Tobisch, Z. Kristallogr. **118**, 473 (1963).

[35] *The Hall Effect and Its Applications*, edited by C. L. Chien and C. R. Westgate (Plenum, New York, 1980).

[36] J. M. Luttinger, Phys. Rev. **112**, 739 (1958).

[37] L. Berger, Phys. Rev. B **2**, 4559 (1970).

[38] T. Jungwirth, Q. Niu, and A. H. MacDonald, Phys. Rev. Lett. **88**, 207208 (2002).

[39] A. Crepieux and P. Bruno, Phys. Rev. B **64**, 014416 (2001).

[40] W.-L. Lee, S. Watauchi, R. J. Cava, and N. P. Ong, Science **303**, 1647 (2004).

[41] P. Matl, N. P. Ong, Y. F. Yan, Y. Q. Li, D. Studebaker, T. Baum, and G. Doubinina, Phys. Rev. B **57**, 10248 (1998).

[42] T. Holstein, Phys. Rev. **124**, 1329 (1961).

[43] Y. Imry, Phys. Rev. Lett. **71**, 1868 (1993).

[44] Y. Lyanda-Geller, S. H. Chun, M. B. Salamon, P. M. Goldbart, P. D. Han, Y. Tomioka, A. Asamitsu, and Y. Tokura, Phys. Rev. B **63**, 184426 (2001).

[45] S. R. Shinde, S. B. Ogale, J. S. Higgins, H. Zheng, A. J. Millis, V. N. Kulkarni, R. Ramesh, R. L. Greene, and T. Venkatesan, Phys. Rev. Lett. **92**, 166601 (2004).